ON THE MECHANICAL BEHAVIOUR OF MONOFILAMENT TECHNICAL TEXTILES

Valter Carvelli

Department of Structural Engineering, Technical University (Politecnico) of Milan
Piazza Leonardo Da Vinci 32, 20133 Milan, Italy
valter.carvelli@polimi.it

ABSTRACT

In this work the mechanical behaviour of dry monofilament technical textiles is investigated. The considered textiles are typically used in the screen printing industry. In this and other fields, the deformability of the textile is an essential aspect for the quality of the final product. Therefore, a full knowledge of the mechanical properties of the textile is mandatory to predict the influence of several aspects. The mechanical behaviour of the monofilament textiles is here studied by means of numerical analyses of different representative volume (RV) geometries. Two different monofilament polyester plain-weave textiles were examined. For both textiles, the three-dimensional finite element models of two RVs were produced. The validation of the proposed numerical approach was conducted comparing the numerical results to the experimental observations for the two textiles during different loading conditions.

1. INTRODUCTION

The mechanical behaviour of textiles is often of great importance in several industrial applications. This is the case for textile reinforcement used in composites or for technical textiles [1]. The forming of the textile preform in a composite component or the correct ink deposition in a screen printing application depend on the tensile response in the principal directions and on the shear behaviour of the fabric.

The experimental determination of this mechanical feature is time consuming and requires tools and procedures not completely standardized. Reliable models are extremely important for the prediction of the mechanical properties of textiles in particular for their non-linear behaviour.

Many of the available analytical [2] and numerical [3] models are devoted to the textile reinforcement used in composites. The mechanical response of monofilament textiles is mainly predicted by analytical model [4].

In this work a numerical approach for predicting the mechanical behaviour of monofilament technical textiles is presented. The numerical analysis is restricted to the textiles representative volume (RV) following an approach applied to textile composite materials [5]. The three-dimensional geometry of the RV was reproduced on the basis of the measures obtained from microscopic digital pictures. Two different representative volumes extracted from a plane weave monofilament textile are used in the numerical simulations.

The numerical analyses on the RVs produce the mechanical parameters of an hypothetical homogeneous material equivalent, from the mechanical point of view, to the original textile. The macroscopic equivalence between the original and the fictitious homogeneous textiles could be assessed by the homogenization theory for periodic media. This fictitious homogeneous material may be used in the numerical modelling of textile components (see e.g. [6]).

The numerical investigation is limited to two different monofilament polyester plain-weave textiles for which an extensive experimental campaign was performed by the author and co-workers [6, 7]. The considered textiles differ for the nominal fibre diameter (34 and 64μm) and for the fibre density (150 and 62 fibres/cm).

2. A BRIEF OVERVIEW OF THE EXPERIMENTAL TESTS

Two monofilament technical textiles were investigated (called in the following A and B). Both textiles present a typical plain weave geometry formed interlacing polyester fibres with the same geometry in two perpendicular directions. The geometric features reported in Table 1 are the nominal geometric values provided by the producer equal in the warp and weft direction. The fabrics differ in the fibre diameters and in the number of fibres per unit length.

Textile	Nominal fibres diameter [μm]	Number of fibres per cm
A	34	150
B	64	62

Table 1. Nominal features of the monofilament technical textiles.

The experimental activities began with the measurement of the textiles geometry in order to reproduce numerical models as close as possible to real ones. Several samples of the textiles were observed [6]. A microscope was used to measure the geometry of the yarns and the distance between the fibres (see Figure 1). A Scanning Electronic Microscope (SEM) was used to estimate the ovalization of the fibre cross sections measuring the maximum (D_{max}) and minimum (D_{min}) diameters. The average values of the geometrical measurements are reported in Table 2.

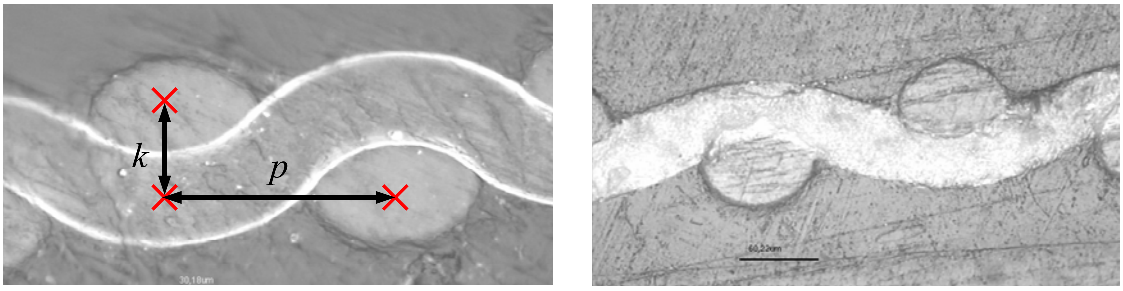

(a) (b)

Figure 1. Cross-section of textile (a) A and (b) B in the warp direction.

Textile	Direction	*k* [μm]	*p* [μm]	D_{nom} [μm]	D_{max} [μm]	D_{min} [μm]
A	warp	24.3	67	34	44.92	34.01
	weft	28.5	67	34	42.67	37.97
B	warp	47.8	161	64	73.22	55.81
	weft	53.9	161	64	77.83	65.04

Table 2. Geometrical measured features of the textiles.

The experimental activities were carried out both on single fibres and textile specimens. Tensile tests were performed on the fibres while both uniaxial and biaxial tensile tests were carried out on specimens of the textiles. The tractions on fibres were performed using a uniaxial testing machine MTS Synergie 200H equipped with a load cell with maximum capacity of 100N. The uniaxial and biaxial tensile tests on textiles were carried out using an home-made device (see Figure 2) equipped with two independent orthogonal axes [6, 7].

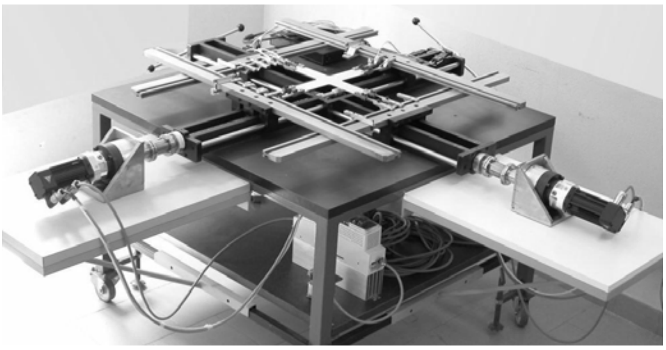

Figure 2. Biaxial tensile device.

The different behaviour of the fibres before and after the weaving process suggests to use, in the numerical analyses as average constitutive behaviour, the tensile properties of the fibres extracted from the textiles. The specimen preparation and the tensile tests were carried out in accordance to the standards ASTM D 3822–96. Some typical stress–strain curves of the fibres are reported in Figure 3. The stress was evaluated using the nominal cross-section, while the strain was recorded during the experiments on a base length of 200mm.

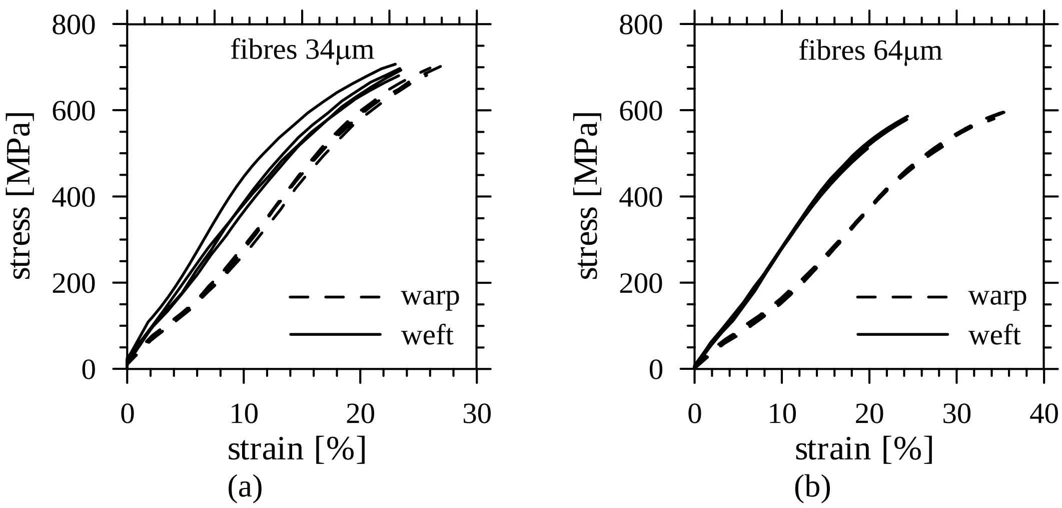

Figure 3. Experimental tensile tests of fibres extracted from textiles. Stress vs. Strain of the fibres with diameter (a) 34 μm and (b) 64 μm

The biaxial tensile tests on the textiles were performed using a cruciform specimen (see Figure 4). A set of markers was reported in the central part of the specimen. The displacements of the markers during the loading process were recorded by means a digital camera. The post processing of the digital images was carried out by a specific software that provides the maps of the displacements in the central area of the specimen. Fitting the displacement measurements at the marker points by bi-quadratic functions, the Green-Lagrange strain components were evaluated [7]. Some maps of the strain components at failure of a textile A specimen under biaxial loading are depicted in Figure 5.

The uniaxial tensile tests were carried out in accordance to the standards ASTM D 5035-95. Rectangular specimens were cut, 50 mm wide and 300mm length. Different sets of specimens were prepared to orient the load at 0^o, 90^o and 45^o to the warp fibres direction.
For an exhaustive description of the experimental campaign see [6].

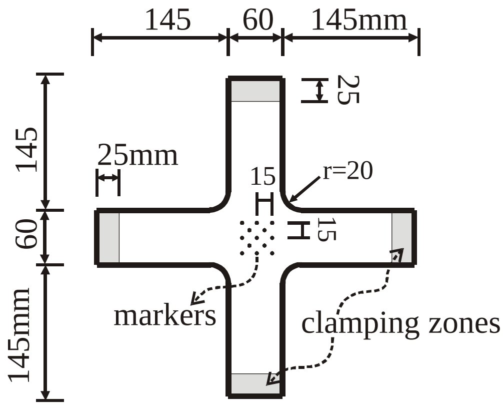

Figure 4. Geometry of the specimen for biaxial test.

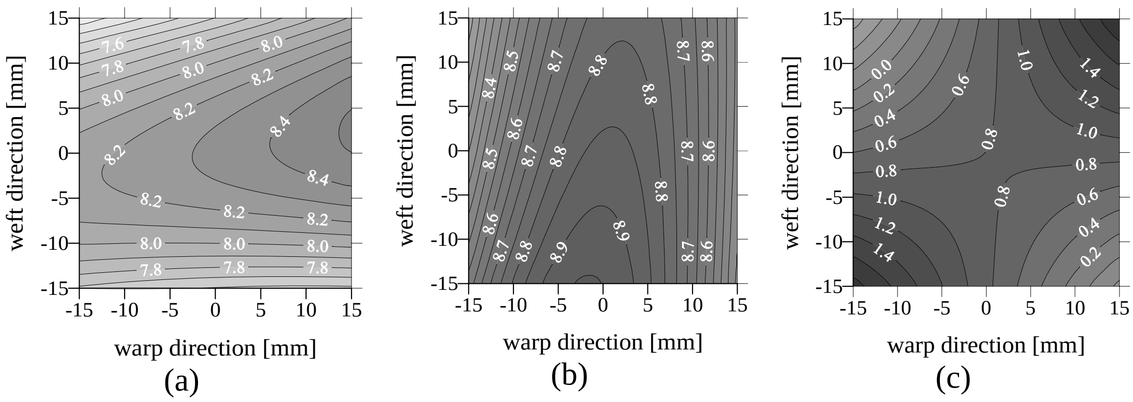

Figure 5. Maps of the strain components at failure in a textile A specimen centre zone: (a) strain in the warp direction; (b) strain in the weft direction; (c) shear strain in the textile plane.

3. THE NUMERICAL MODELS

To predict the influence of some geometrical and fibres features on the global and local mechanical behaviour of monofilament technical textiles, three-dimensional finite element models were implemented.
Assuming the regular distribution of the fibres in the textile plane (see Figure 6), the numerical models are limited to a periodic representative volume. In this paper the two considered periodic RVs are depicted in Figure 7, for a plane weave textile.
From the numerical results of the RV analysis, the macroscopic (global) properties of the equivalent material are evaluated by averaging the quantities on the RV volume [8].
The representative volume was modelled using the geometrical quantities measured on the specimens of the two textiles (see Table 2). The longitudinal shapes of the fibres in the RV were defined fitting the microscope measurements with a trigonometric function. The transversal cross section of the fibres were assumed with elliptic shape, adopting the data in Table 2, and was kept constant in the fibre longitudinal direction.

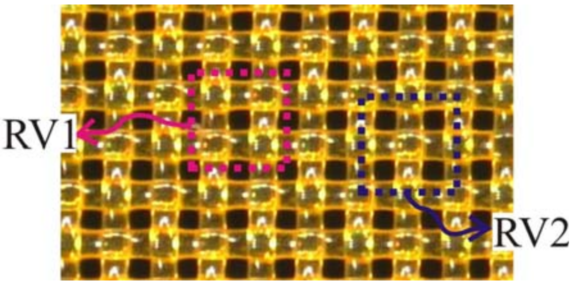

Figure 6. A plane weave textile and two periodic representative volumes.

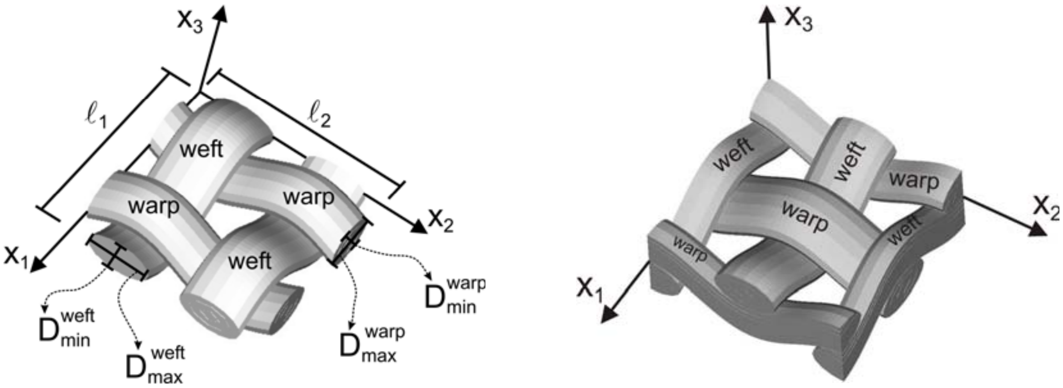

RV1 RV2

Figure 7. Geometrical sketch of the two representative volumes (RV1 and RV2) and some geometrical parameters.

To reproduce the textile periodicity (hypothesis of regular distribution of the fibres in the textile), the following kinematic boundary conditions were imposed to the finite element model of the RV (see also [5]) in term of the displacement vector $\underline{u}$:

$$\underline{u}_A - \underline{u}_B = \underline{\underline{E}}(\underline{x}_A - \underline{x}_B) \quad (1a)$$

$$\underline{u}_C - \underline{u}_D = \underline{\underline{E}}(\underline{x}_C - \underline{x}_D) \quad (1b)$$

where A and B are two points of a weft fibre on the cross section x_1=0 and $x_1=\ell_1$ corresponding in the periodicity; C and D are two points of a warp fibre on the cross section x_2=0 and $x_2=\ell_2$ corresponding in the periodicity (see Figure 7). In eqn. (1) $\underline{\underline{E}}$ represents the macroscopic strain tensor.

Additional kinematic conditions are enforced to avoid penetration between fibres and the friction in the fibre-fibre contacts by Coulomb's model.

The finite element meshes of the two RVs were built with four nodes tetrahedral elements C3D4 [8]. The features of the meshes are listed in Table 3.

Textile	**RV**	**Node num.**	**Element num.**
A	RV1	6380	25920
	RV2	5330	19200
B	RV1	6612	26880
	RV2	7410	26880

Table 3. Features of the RVs finite element meshes.

The Ramberg-Hosgood nonlinear constitutive model [9] was used to reproduce the fibre materials mechanical behaviour. The uniaxial Ramberg-Hosgood's stress-strain (σ-ε) equation is:

$$E\varepsilon = \sigma\left(1 + \alpha\left(\frac{|\sigma|}{\sigma_0}\right)^{n-1}\right) \qquad (2)$$

The parameters involved in the Ramberg-Hosgood model (E, α, n, σ_0) were obtained fitting the experimental data obtained with the tensile tests on the fibres (Figure 3), see in [6] for their values.

4. NUMERICAL AND EXPERIMENTAL COMPARISONS

The numerical predictions obtained with the two representative volumes of a monofilament plane weave textile, are compared to the experimental observations for the two textiles up to failure. The ultimate failure was defined comparing the maximum average Mises's equivalent stress of the fibres cross-sections with the experimental ultimate tensile stress of the fibres (Figure 3). For a fibre cross-section, the average of the Mises's stress was evaluated considering the stress value in the integration points of the finite elements contained in it.

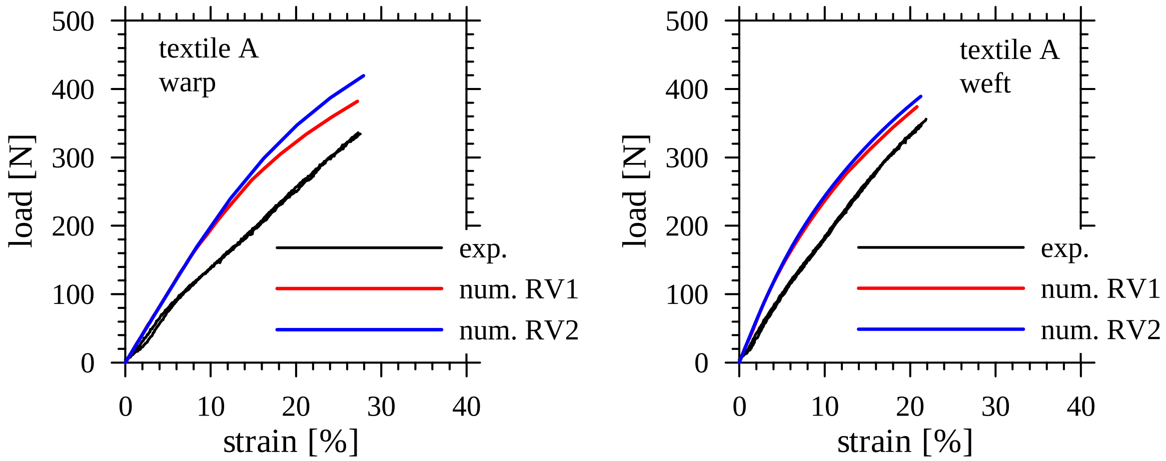

(a) (b)

Figure 8. Uniaxial tensile test: Textile A in (a) warp and (b) weft directions.

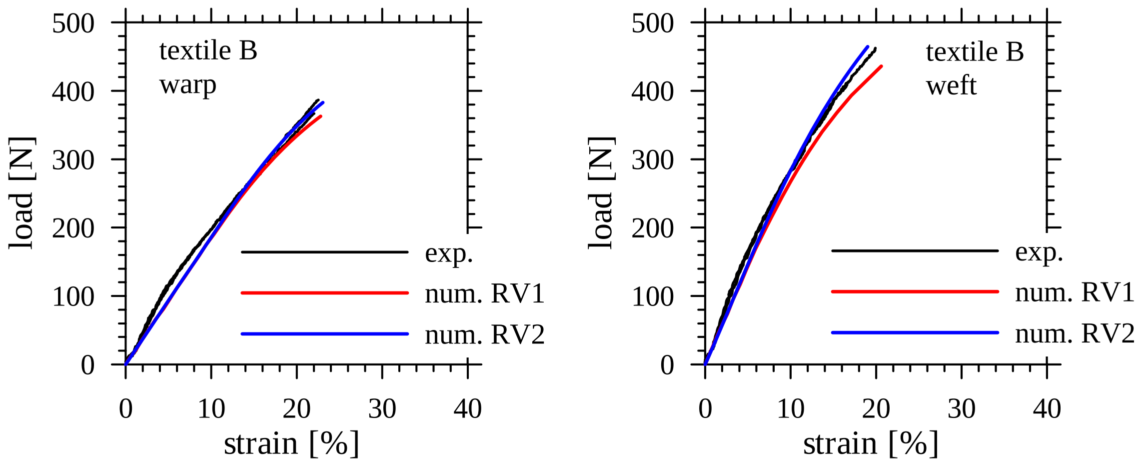

(a) (b)

Figure 9. Uniaxial tensile test: Textile B in (a) warp and (b) weft directions.

The numerical macroscopic mechanical responses of the two RVs subject to uniaxial traction in warp and weft directions are depicted in Figure 8 and Figure 9. The numerical macroscopic load vs. strain (in the load direction) curves show very similar predictions assuming the two different representative volumes. The comparison with the uniaxil experimental tests gives a satisfactory indication on the accuracy of the mumerical models for this load condition (Figure 8 and Figure 9).
The numerical results of the biaxial simulations for both RVs are reported in Figure 10 in terms of force vs. strain curves for both textiles A and B. The comparisons of numerical and experimental curves shows an underestimation of the textile stiffness by the numerical models.
The stress concentration zones and the local deformations of the fibres can be estimated from the FE models results. In Figure 11 the undeformed and deformed shapes of the two representative volumes FE models of textile A are depicted in the biaxial tensile loading. These pictures could be useful to predict the influence of the material properties and the geometry of the fibres on the size of the ink drops or the resin flow through the textile.

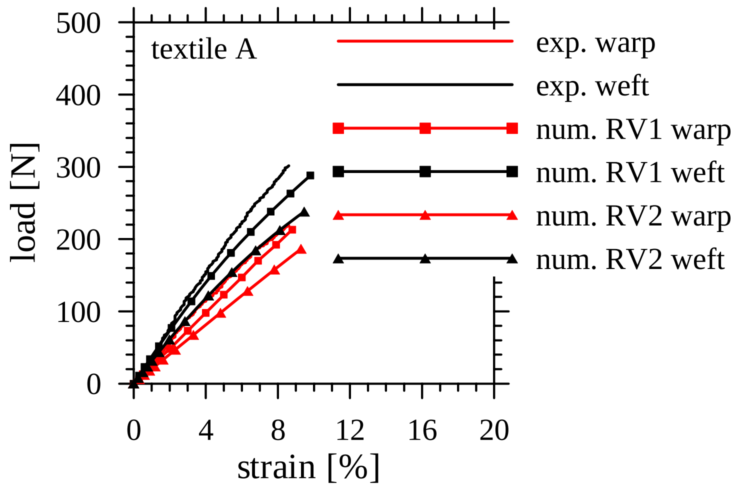

(a)

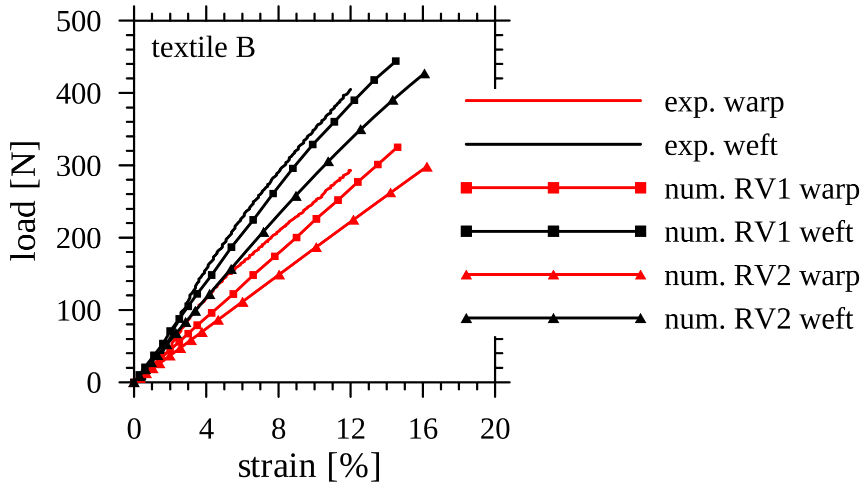

(b)

Figure 10. Biaxial tensile test: (a) Textile A and (b) Textile B.

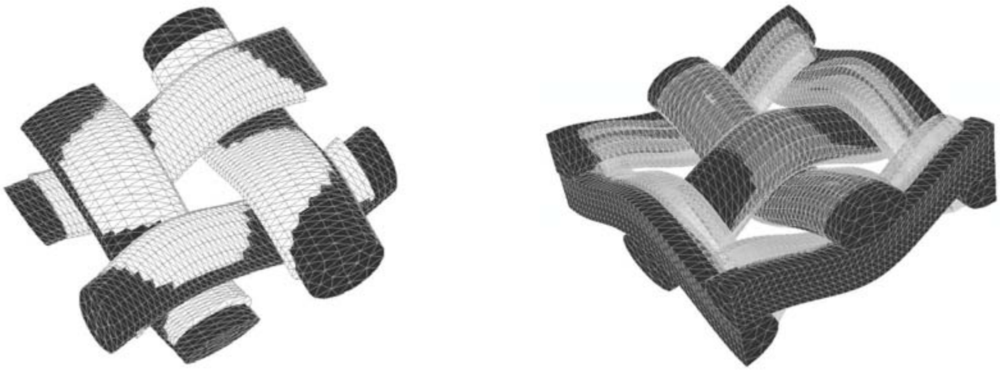

RV1 RV2

Figure 11. Biaxial tensile test of the textile A: undeformed (white) and deformed (black) geometry of the RV1 and RV2 FE models.

5. CONCLUSIONS

The numerical models presented allow to study the mechanical properties of monofilament plain weave textiles. The approach is based on the finite element discretization of the textile representative volume. The numerical results based on two different shapes of the representative volume show very similar responses in particular for the unixail tensile behaviours. The numerical predictions of the textiles mechanical behaviour, when subjected to uniaxial or biaxial tractions, are in a satisfactory agreement with the experimental data.

ACKNOWLEDGEMENT. The author thanks Pietro Campagna for his help in numerical computations.

REFERENCES

1 Long A. C., "Design and manufacture of textile composites", Woodhead Publishing Ltd., 2005.
2 Lomov S. V., Verpoest I., "Model of shear fabric and parametric description of shear resistance of glass woven reinforcements". *Composites Science and Technology*, 2006;66: 919-933.
3 Badel P., Vidal-Sallé E., Boisse P., "Computational determination of in-plane shear mechanical behaviour of textile composite reinforcements". *Computational Materials Science*, 2007;40: 439-448.
4 Kawabata S., Masako Niwa M., Kawai H., "The finite-deformation theory of plane-weave fabrics. Part II: The shear deformation theory". *Journal of Textile Institute*, 1973;64: 61-85.
5 Carvelli V., Poggi C., "A homogenization procedure for the numerical analysis of woven fabric composites". *Composite Part A*, 2001;32: 1425-1432.
6 Carvelli V., Corazza C., Poggi C., "Mechanical modelling of monofilament technical textiles". *Comp. Mat. Science*, in print, doi:10.1016/j.commatsci.2007.10.003.
7 Quaglini V., Corazza C., Poggi C., "Experimental characterisation of orthotropic technical textiles under uniaxial and biaxial loading", *Composites Part A*, in print, doi:10.1016/j.compositesa.2007.07.008.
8 Nemat-Nasser, M. Hori, Micromechanics: Overall Properties of Heterogeneous Solids, *Elsevier Science Publishers*, 1999.
9 ABAQUS Standard User's Manual, ver. 6.6, Hibbit, Karlsson & Sorensen Inc., 2006.